

could be an important factor in their association with some neurodegenerative diseases (15) and might allow their dissociation into oligomers, which can interact with cellular components. The differences between the moduli of mature amyloid fibrils and HbS fibrils further highlight the different balance of inter- versus intramolecular interactions. Thus, in both cases, a sizable fraction of residues participates in hydrogen bonds: within  $\alpha$  helices for HbS and within  $\beta$  sheets for amyloid fibrils. However, for HbS fibrils, these bonds are all within one individual molecule, and the intermolecular interactions are mediated by weaker surface interactions; on the other hand, for amyloid fibrils, some or all of the hydrogen bonds are intermolecular when they can contribute to the long-range stability of the fibril and the high elastic modulus. These conclusions are exemplified by the orb-weaving spider's use of two forms of silk. Dragline silk, which contains a high fraction of densely hydrogen-bonded domains, is used to provide the structural scaffold for the web (27) and has an elastic modulus that is comparable to hydrogen-bonded cross- $\beta$  protein nanofibrils (Fig. 2). On the other hand, web capture silk, which serves for arresting prey, is a viscid biofilament containing cross-linked polymer networks and has an elastic modulus that is comparable to that of elastomers such as rubber and elastin (27).

The finding that the rigidity of amyloid fibrils is described by a common elastic modulus, defined predominantly by intermolecular interactions involving the common polypeptide main chain, provides quantitative evidence for the idea (2) that these structures

form a generic class of material. In addition, our results provide insight into the changes in the distribution of inter- versus intramolecular bonding interactions associated with the transition of proteins from their native globular structures into polymeric supramolecular assemblies. Finally, comparisons between artificial self-assembling protein fibrils and natural cellular structures exemplify the design criteria used in nature to select materials for structural applications and provide inspiration for the design of novel nanoscale biomaterials.

#### References and Notes

- D. M. Fowler, A. V. Koulov, W. E. Balch, J. W. Kelly, *Trends Biochem. Sci.* **32**, 217 (2007).
- F. Chiti, C. M. Dobson, *Annu. Rev. Biochem.* **75**, 333 (2006).
- M. Tanaka, S. R. Collins, B. H. Toyama, J. S. Weissman, *Nature* **442**, 585 (2006).
- D. M. Fowler *et al.*, *PLoS Biol.* **4**, e6 (2005).
- S. Zhang, *Nat. Biotechnol.* **21**, 1171 (2003).
- S. Zhang, T. Holmes, C. Lockshin, A. Rich, *Proc. Natl. Acad. Sci. U.S.A.* **90**, 3334 (1993).
- F. Gelain, D. Bottai, A. Vescovi, S. Zhang, *PLoS ONE* **1**, e119 (2006).
- T. Scheibel *et al.*, *Proc. Natl. Acad. Sci. U.S.A.* **100**, 4527 (2003).
- M. Sunde *et al.*, *J. Mol. Biol.* **273**, 729 (1997).
- C. M. Dobson, *Trends Biochem. Sci.* **24**, 329 (1999).
- Materials and methods are available as supporting material on *Science Online*.
- J. C. Wang *et al.*, *J. Mol. Biol.* **315**, 601 (2002).
- T. P. J. Knowles, J. F. Smith, A. Craig, C. M. Dobson, M. E. Welland, *Phys. Rev. Lett.* **96**, 238301 (2006).
- J. F. Smith, T. P. J. Knowles, C. M. Dobson, C. E. Macphee, M. E. Welland, *Proc. Natl. Acad. Sci. U.S.A.* **103**, 15806 (2006).
- P. T. Lansbury, H. A. Lashuel, *Nature* **443**, 774 (2006).
- S. Sambashivan, Y. Liu, M. R. Sawaya, M. Gingery, D. Eisenberg, *Nature* **437**, 266 (2005).

17. T. Lührs *et al.*, *Proc. Natl. Acad. Sci. U.S.A.* **102**, 17342 (2005).

18. N. Ferguson *et al.*, *Proc. Natl. Acad. Sci. U.S.A.* **103**, 16248 (2006).

19. M. R. Sawaya *et al.*, *Nature* **447**, 453 (2007).

20. R. Nelson *et al.*, *Nature* **435**, 773 (2005).

21. L. Esposito, C. Pedone, L. Vitagliano, *Proc. Natl. Acad. Sci. U.S.A.* **103**, 11533 (2006).

22. R. J. Hawkins, T. C. B. McLeish, *Phys. Rev. Lett.* **93**, 098104 (2004).

23. T. Haliloglu, I. Bahar, B. Erman, *Phys. Rev. Lett.* **79**, 3090 (1997).

24. J. Park, B. Kahng, R. D. Kamm, W. Hwang, *Biophys. J.* **90**, 2510 (2006).

25. A. Kis *et al.*, *Phys. Rev. Lett.* **89**, 248101 (2002).

26. F. Gittes, B. Mickey, J. Nettleton, J. Howard, *J. Cell Biol.* **120**, 923 (1993).

27. F. Vollrath, D. Porter, *Soft Matter* **2**, 377 (2006).

28. M. F. Ashby, D. R. H. Jones, *Engineering Materials: An Introduction to Their Properties and Applications* (Pergamon, Oxford, ed. 1, 1980).

29. J. Käs, H. Strey, E. Sackmann, *Nature* **368**, 226 (1994).

30. Single-letter abbreviations for the amino acid residues are as follows: A, Ala; C, Cys; D, Asp; E, Glu; F, Phe; G, Gly; H, His; I, Ile; K, Lys; L, Leu; M, Met; N, Asn; P, Pro; Q, Gln; R, Arg; S, Ser; T, Thr; V, Val; W, Trp; and Y, Tyr.

31. We acknowledge helpful discussions with E. Terentjev, R. Hawkins, S. Rogers, and J. Smith, as well as financial support from the Engineering and Physical Sciences Research Council and the Interdisciplinary Research Collaboration in Nanotechnology. We thank S. Shammas, A. Brorsson, and G. Devlin for preparing the  $\text{A}\beta$  and TTR fibrils, and A. Tickler for synthesizing the TTR peptide. The work of C.M.D is supported, in part, by Programme Grants from the Wellcome Trust and the Leverhulme Trust.

#### Supporting Online Material

[www.sciencemag.org/cgi/content/full/318/5858/1900/DC1](http://www.sciencemag.org/cgi/content/full/318/5858/1900/DC1)  
Materials and Methods

Figs. S1 and S2

References

4 September 2007; accepted 9 November 2007  
10.1126/science.1150057

## A Sulfur Dioxide Climate Feedback on Early Mars

Itay Halevy,<sup>1\*</sup> Maria T. Zuber,<sup>2</sup> Daniel P. Schrag<sup>1</sup>

Ancient Mars had liquid water on its surface and a  $\text{CO}_2$ -rich atmosphere. Despite the implication that massive carbonate deposits should have formed, these have not been detected. On the basis of fundamental chemical and physical principles, we propose that climatic conditions enabling the existence of liquid water were maintained by appreciable atmospheric concentrations of volcanically degassed  $\text{SO}_2$  and  $\text{H}_2\text{S}$ . The geochemistry resulting from equilibration of this atmosphere with the hydrological cycle is shown to inhibit the formation of carbonates. We propose an early martian climate feedback involving  $\text{SO}_2$ , much like that maintained by  $\text{CO}_2$  on Earth.

Martian geomorphology indicates the existence of liquid surface water, perhaps even an ocean (1), during the late Noachian epoch [ $\sim 3.8 \times 10^9$  years ago (2)], when surface temperatures were marginally above freezing (3) but still considerably warmer than at present. The climatic conditions are most likely explained by an optically thicker atmospheric greenhouse (4) that may also have had to compensate for a dimmer sun (5). A  $\text{CO}_2$ -rich atmosphere could have been supplied by vigorous volcanism associated with the

emplacement of the Tharsis igneous province (6) as well as with earlier episodes of crustal formation. Although attempts at explaining the existence of liquid water with an atmosphere of pure  $\text{CO}_2$  are complicated by  $\text{CO}_2$  condensation (7), the possible existence of infrared-reflective  $\text{CO}_2$  ice clouds (8) or atmospheric heating due to absorption of solar radiation by trace amounts of  $\text{SO}_2$  (9) has been suggested to resolve this difficulty.

If early volcanic activity on Mars did sustain a thick  $\text{CO}_2$  atmosphere, one might expect the

existence of a carbon cycle similar to Earth's, where the release of  $\text{CO}_2$  from volcanoes is balanced by burial of calcium carbonate through silicate weathering reactions that remove protons and release alkalinity to seawater (10). The dependence of silicate weathering on temperature and precipitation creates a negative feedback on the atmospheric abundance of  $\text{CO}_2$ , stabilizing the climate to maintain surface conditions with adequate liquid water for weathering as long as the volcanic release of  $\text{CO}_2$  continues. Existence of such a carbon cycle on Mars would have left carbonate sediments at the surface as well as abundant clays left over from the weathering process. For example, a carbon outgassing flux of  $7 \times 10^{12} \text{ mol C year}^{-1}$ , about the same as the modern volcanic outgassing rate on Earth (11), maintained for  $10^8$  years would result in a global carbonate layer  $\sim 180 \text{ m}$  thick. The same mass of carbonate precipitated in an ocean covering 30% of Mars (1) would form a layer  $\sim 600 \text{ m}$  thick.

<sup>1</sup>Department of Earth and Planetary Sciences, Harvard University, Cambridge, MA 02138, USA. <sup>2</sup>Department of Earth, Atmospheric, and Planetary Sciences, Massachusetts Institute of Technology, Cambridge, MA 02139, USA.

\*To whom correspondence should be addressed. E-mail: ihalevy@fas.harvard.edu

The virtual absence of carbonate minerals above the detection limit of a few weight percent (12), coincident with evidence for an early climate warm enough for liquid water, is therefore puzzling.

A possible resolution of this contradiction may involve the abundance of sulfur on the surface of Mars. Martian soil and rock analyses show significant enrichment in sulfur relative to terrestrial soils (13); recent analysis of data obtained by the rovers identified soils with sulfur contents as high as 7.5 weight %  $\text{SO}_3$  (14). Like carbon, sulfur in some forms can play an important role in radiative forcing and in silicate weathering. In this paper, we explore the implications of an active sulfur cycle, linked to the carbon cycle, on the climate and surface chemistry of early Mars.

In an early martian sulfur cycle, volcanic outgassing of sulfur to the atmosphere and surface environment, primarily as  $\text{SO}_2$  and  $\text{H}_2\text{S}$ , would be balanced by photochemical sinks and precipitation of sulfur-bearing minerals. The modern martian atmosphere is relatively oxidized after billions of years of hydrogen escape (15), although earlier in martian history oxygen escape (16) as well as emission of reduced gases from hydrothermal alteration of basaltic crust (17) likely resulted in a more reducing atmosphere. During the emplacement of Tharsis as with any period of high, sustained volcanism, the additional emission of reduced gases, including  $\text{H}_2\text{S}$  and  $\text{SO}_2$ , would drive the oxidation state even lower. The lifetime of sulfur species that today are rapidly oxidized in Earth's atmosphere is longer under such conditions. In the absence of biological catalysis, kinetic barriers to changes in the valence state of sulfur would enable the coexistence of atmospheric and aquatic sulfide ( $\text{S}^{2-}$ ), sulfite ( $\text{S}^{4+}$ ), and sulfate ( $\text{S}^{6+}$ ) in proportions depending on the relative magnitudes of their sources and sinks.

In an atmosphere with significant quantities of reduced sulfur gases,  $\text{SO}_2$  would play a particularly important role, not only climatically as a powerful greenhouse gas but also in the chemistry of the surface environment.  $\text{SO}_2$  is highly soluble in water, so its early martian geochemical cycle would have been dominated by aquatic reservoirs, such as a northern hemisphere ocean (1) or regions of sustained groundwater upwelling (18). The presence of even a small amount of  $\text{SO}_2$  in a  $\text{CO}_2$ -rich atmosphere lowers the pH of surface waters, suppressing carbonate precipitation in favor of sulfite minerals. The resulting geochemical cycle is analogous to the terrestrial carbon cycle (10), with a silicate weathering feedback on climate involving  $\text{SO}_2$  instead of  $\text{CO}_2$  and the pH of water bodies buffered by the solubility of sulfite minerals and the partial pressure of  $\text{SO}_2$  instead of the solubility of calcite and the partial pressure of  $\text{CO}_2$ .

Details of this geochemical cycle depend on relative rates of sulfur outgassing, photochemical transformations, silicate weathering, and mineral precipitation. Sulfur outgassing from Tharsis is limited by the solubility of sulfur in basaltic melts. The sulfur content of martian melts has recently been estimated at 1400 parts per million (ppm)

(19), one to three times the concentration in Hawaiian lavas (20). Degassing of the entire volume of Tharsis magma [ $3 \times 10^8 \text{ km}^3$  (6)] implies a maximum flux of  $\sim 4 \times 10^{11} \text{ mole S year}^{-1}$  if the emplacement of Tharsis took  $10^8$  years. This is about twice the present sulfur outgassing flux on Earth [ $\sim 13 \times 10^6 \text{ metric tons SO}_2 \text{ year}^{-1}$  (21)], although its impact on the surface of Mars would have been much greater given the smaller volume of the atmosphere. Because the speciation of sulfur coming from volcanic outgassing depends on the oxygen fugacity of the magma, the oxidation state of martian basalts (22) implies that at least 50% of the sulfur, or  $\sim 2 \times 10^{11} \text{ mole S year}^{-1}$ , was emitted as  $\text{H}_2\text{S}$  (23).

Removal of  $\text{SO}_2$  from the atmosphere normally occurs by gas-phase oxidation, by reaction pathways after photolysis, and by a variety of physical sinks leading to deposition and subsequent oxidation. The reducing power from volcanic fluxes of  $\text{H}_2\text{S}$  and  $\text{SO}_2$  described above, combined with hydrothermal emission of hydrogen and methane, would compensate for even the most optimistic estimates of hydrogen escape [summarized in (16)], implying decreased gas-phase oxidation of  $\text{SO}_2$  (24). Furthermore, deposition of  $\text{SO}_2$ , typically followed by rapid heterogeneous oxidation, would instead lead to saturation of the martian surface and return fluxes to the atmosphere at steady state (25). Aqueous disproportionation of sulfite could potentially prevent saturation of the aquatic reservoir with species of  $\text{S}^{4+}$  (26). However, the rates of these reactions in the absence of biological catalysis have only been examined above  $100^\circ\text{C}$  (27) and are likely slow at low temperature [Supporting Online Material (SOM) text].

It has been suggested that reaction of the products of  $\text{SO}_2$  photolysis with atmospheric oxidants recycles  $\text{SO}_2$ , resulting in little net loss (28). However, a low abundance of oxidants limits these reactions as well, introducing another potentially important sink:  $\text{SO}_2$  photolysis followed by disproportionation to sulfate and elemental sulfur (29). This sink was likely also of low magnitude under early martian conditions, because a higher ultraviolet flux attributed to the young Sun (30) would have occurred in wavelengths where absorption and Rayleigh scattering by a thick  $\text{CO}_2$  atmosphere afforded significant shielding (31). Moreover, absorption by the abundance of sulfur volatiles, including  $\text{S}_8$  possibly generated by  $\text{SO}_2$  photochemistry (25), would have further attenuated the energy available for  $\text{SO}_2$  photodissociation (fig. S1). Wong *et al.* (2003) (32) simulated the local atmospheric chemical impact of a volcanic event on the present oxidizing martian atmosphere, calculating a mixing ratio of more than 100 ppm  $\text{SO}_2$  in the lower 60 km of the atmosphere and a very low photolysis rate constant of  $6.1 \times 10^{-18} \text{ s}^{-1}$  at an altitude of 10 km. During the emplacement of Tharsis, a volcanic flux several orders of magnitude higher, sustained over hundreds of millions of years, means that the photolysis sink was unlikely to be of primary importance.

Accumulation of  $10^{-6}$  to  $10^{-4}$  bars of  $\text{SO}_2$  in a  $\text{CO}_2$ -rich atmosphere, made possible by its small total photochemical sink and by saturation of the surface, would have had a substantial radiative effect (33), perhaps enough to have maintained liquid water on the surface of early Mars. Under such conditions, temperature and precipitation are much more sensitive to changes in the partial pressure of  $\text{SO}_2$  ( $p\text{SO}_2$ ) than to changes in the

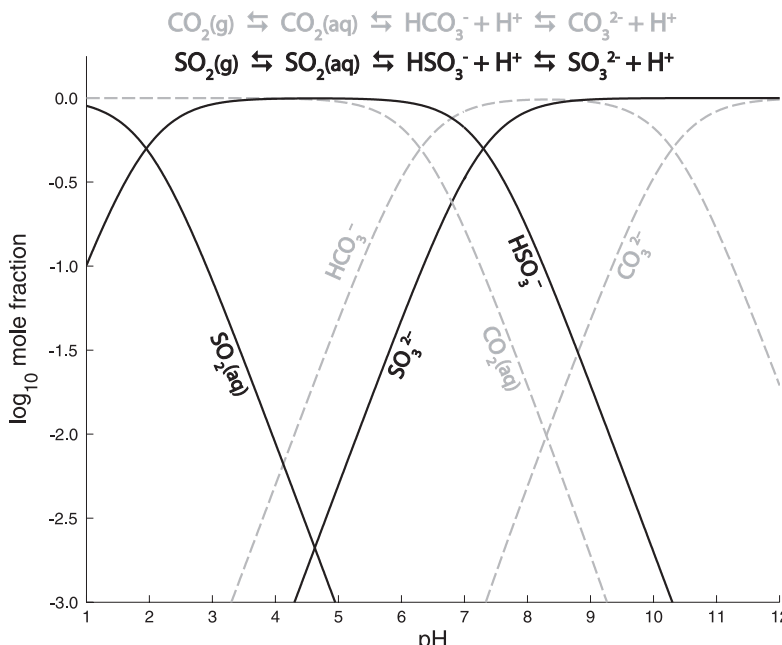


**Fig. 1.** pH dependence of aqueous  $\text{S}^{4+}$  (black) and C (gray) speciation, expressed by the chemical equilibrium reactions in the figure. At pH between 2 and 6, most of the  $\text{S}^{4+}$  is present as  $\text{HSO}_3^-$  (bisulfite), whereas carbon is predominantly in the form of  $\text{CO}_2$  (aq).

partial pressure of  $\text{CO}_2$  ( $p\text{CO}_2$ ), mainly because of the large difference between the atmospheric abundances of  $\text{SO}_2$  and  $\text{CO}_2$  but also because of saturation of the infrared absorption lines of  $\text{CO}_2$ . Additionally, because of the high solubility of  $\text{SO}_2$ , most of the  $\text{S}^{4+}$  would have been present in the aquatic reservoir and would have had a dominant role in the surface environment. Because hydration of  $\text{SO}_2$  forms sulfurous acid ( $\text{H}_2\text{SO}_3$ ) ( $\text{H}_2\text{SO}_3$ ), which is much stronger than carbonic acid (34), the pH of water in equilibrium with  $\text{CO}_2$  and  $\text{SO}_2$  is essentially independent of  $p\text{CO}_2$  when  $p\text{SO}_2 > \sim 1 \times 10^{-5}$  bars (fig. S2). With climate and the pH of rainwater controlled pre-

dominantly by the atmospheric abundance of  $\text{SO}_2$ , the rate of silicate weathering in the system we describe would have also responded mainly to changes in  $p\text{SO}_2$ .

Cations released by silicate weathering reactions, electrochemically balanced by bisulfite ( $\text{HSO}_3^-$ ) and bicarbonate ( $\text{HCO}_3^-$ ) anions, are delivered by streams to larger water bodies, eventually resulting in precipitation of salts. Like carbon, the aqueous speciation of  $\text{S}^{4+}$  depends on pH (Fig. 1). Because  $\text{H}_2\text{SO}_3$  is a stronger acid, at low pH the concentration of the sulfite ( $\text{SO}_3^{2-}$ ) anion can be orders of magnitude higher than that of carbonate ( $\text{CO}_3^{2-}$ ), depending on the ratio of

$p\text{SO}_2$  to  $p\text{CO}_2$ . Thermodynamic equilibrium predicts that, for  $p\text{SO}_2/p\text{CO}_2 \geq \sim 5.0 \times 10^{-8}$ , hannebachite ( $\text{CaSO}_3 \cdot \frac{1}{2}\text{H}_2\text{O}$ ) reaches saturation at a lower concentration of  $\text{Ca}^{2+}$  than calcite ( $\text{CaCO}_3$ ). Precipitation of hannebachite then limits the availability of  $\text{Ca}^{2+}$ , suppressing calcite precipitation (Fig. 2) (35). A similar limitation of  $\text{Mg}^{2+}$  availability by  $\text{MgSO}_3 \cdot 6\text{H}_2\text{O}$  precipitation occurs at  $p\text{SO}_2/p\text{CO}_2 \geq \sim 1.2 \times 10^{-4}$ , preventing the precipitation of magnesite ( $\text{MgCO}_3$ ). The actual precipitate may be a mixed Ca-Mg sulfite analogous to dolomite, suppressing magnesite precipitation at an even lower ratio of  $\text{SO}_2$  to  $\text{CO}_2$ . No geologically feasible conditions lead to precipitation of ferrous sulfite instead of highly insoluble siderite ( $\text{FeCO}_3$ ). However, formation of iron-bearing clays as products of basalt alteration (36) as well as precipitation of pyrite ( $\text{FeS}_2$ ) could limit the availability of  $\text{Fe}^{2+}$ , making siderite a minor phase and perhaps preventing its precipitation altogether. We propose that, in an atmosphere rich in  $\text{SO}_2$ , carbonates of iron, magnesium, and calcium rarely form; it is then unnecessary to explain their absence by burial (37), photodisintegration (38), dissolution (39), or destruction via reaction with atmospheric  $\text{SO}_2$  (13). Unlike some of the mechanisms proposed to explain the absence of carbonates (40), suppression of carbonate precipitation by this mechanism occurs even at mildly acidic pH (~6), allowing the formation of clays and consistent with their detection on the ancient martian surface (41).

Without biologically mediated oxidation and reduction of sulfur, cycles of  $\text{S}^{4+}$  and  $\text{S}^{2-}$  would exist alongside the geochemical cycle of  $\text{S}^{4+}$ . Even in a reducing atmosphere, some sulfate would be produced by  $\text{SO}_2$  disproportionation during photochemical reactions. Like acid rain on Earth, this flux of  $\text{H}_2\text{SO}_4$  could slightly depress rainwater pH. However, the pH of water bodies, including a martian ocean, would be buffered by  $p\text{SO}_2$  and sulfite mineral solubility, just as the pH of the surface ocean on Earth is controlled by  $p\text{CO}_2$  and calcite solubility. The main impact of  $\text{H}_2\text{S}$  on the aqueous chemistry of a mildly acidic water reservoir containing iron is the possible contribution of pyrite to the mineral assemblage.

The dependence of weathering rates on atmospheric  $\text{SO}_2$  and the precipitation of sulfite minerals as a sink for  $\text{SO}_2$  create a climate feedback analogous to that involving  $\text{CO}_2$  on Earth; if the volcanic supply of  $\text{SO}_2$  increases, causing atmospheric  $p\text{SO}_2$  to rise, then temperature increases, causing an acceleration of weathering reactions and removal of  $\text{SO}_2$  by precipitation of sulfite minerals, until these balance the increased volcanic supply. Furthermore, the vast reservoir of dissolved  $\text{S}^{4+}$  in the surface aquatic system serves as a buffer to the atmospheric abundance of  $\text{SO}_2$  and would thus stabilize surface temperatures. Relative to the carbonic acid weathering of granitic crust on Earth, the sulfurous acid-driven feedback on the basaltic crust of Mars would be more sensitive to changes in temperature. As a result, the temperature required to

**Fig. 2.** Cation concentration limits imposed by sulfite (black) or carbonate (gray) mineral saturation as a function of  $p\text{SO}_2/p\text{CO}_2$ . **(Top)** Ca mineral saturation and **(bottom)** Mg mineral saturation. The curves are solid in the range of  $p\text{SO}_2/p\text{CO}_2$  in which precipitation of the represented mineral is the limiting factor on cation concentrations. Thin dashed lines mark the critical value of  $p\text{SO}_2/p\text{CO}_2$  above which concentrations are limited by saturation of sulfite rather than carbonate minerals.

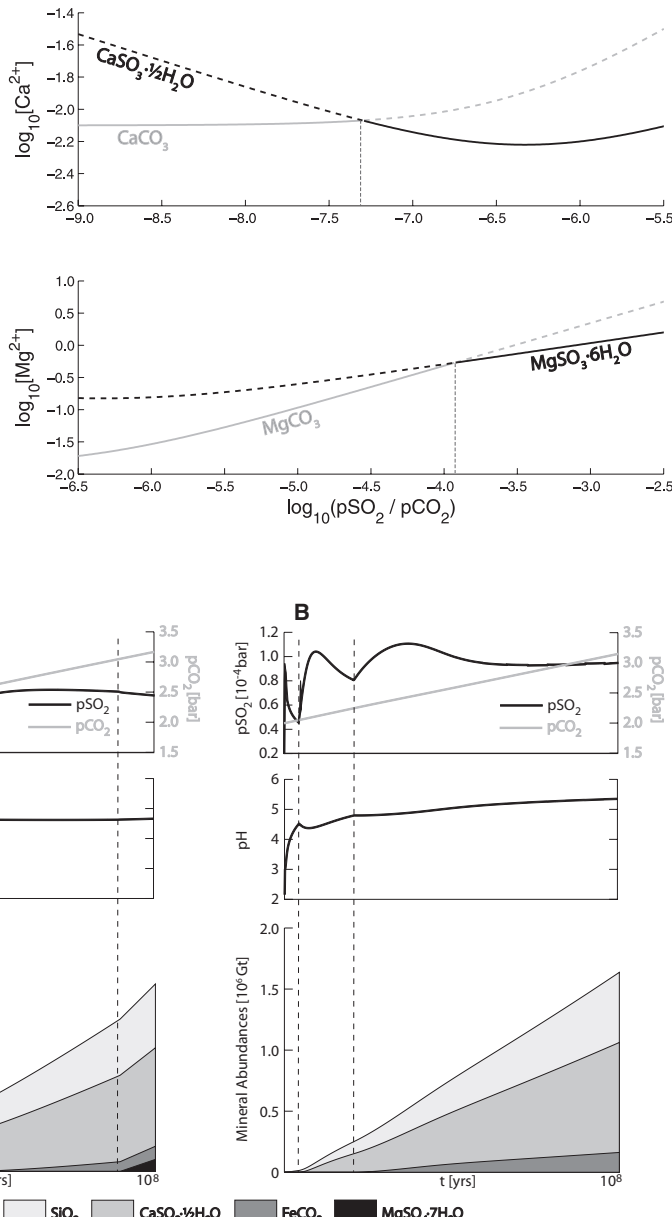


**Fig. 3.** Time ( $t$ ) evolution of  $p\text{SO}_2$ ,  $p\text{CO}_2$  (top), surface water pH (middle), and the precipitated mineral assemblage (bottom), for **(A)** 70% and **(B)** 20% photochemical destruction of all  $\text{SO}_2$  outgassed or produced. The volcanic outgassing rate during this simulation was  $2 \times 10^{11}$  mole year $^{-1}$   $\text{SO}_2$  and  $\text{H}_2\text{S}$ , each. Note that the onset of calcium sulfite and ferrous carbonate precipitation (vertical dashed lines) is accompanied by a decrease in pH because of removal of alkalinity and an increase in  $p\text{SO}_2$  because of water body acidification.

balance  $\text{SO}_2$  outgassing would be relatively low, perhaps just above the temperature necessary to sustain liquid water. This result is consistent with geochemical evidence that Mars in the late Noachian was likely never very warm (3).

To explore this feedback cycle, we constructed a model of the sulfur and carbon cycles of early Mars, including an ocean covering ~30% of the planet, an area about equivalent to the area covered by the *Vastitas Borealis* Formation, inferred to be of aqueous sedimentary origin (1). The model tracks the evolution of the surface (42) reservoirs of carbon, the sulfur in its different valence states, and the dissolved reservoirs of weathering-derived cations and  $\text{SiO}_2$ . Carbon is supplied by volcanic emission of  $\text{CO}_2$  and removed by carbonate mineral precipitation.  $\text{SO}_2$  ( $\text{S}^{4+}$ ) and  $\text{H}_2\text{S}$  ( $\text{S}^{2-}$ ) are also volcanically outgassed and are removed from the surface reservoir by either mineral precipitation or photochemical transformations, leading to formation and deposition of elemental sulfur ( $\text{S}^0$ ) or sulfate ( $\text{S}^{6+}$ ). Cations are supplied to the ocean by silicate weathering, a function of  $p\text{CO}_2$ ,  $p\text{SO}_2$ , and the photochemical production of  $\text{H}_2\text{SO}_4$ . Minerals may precipitate if concentrations of their dissolved components exceed experimentally determined degrees of supersaturation. Aqueous disproportionation of sulfite was not considered in the model because of its sluggish kinetics at low temperature. Further model details are in the SOM text.

Simulated  $p\text{SO}_2$ , pH, and precipitated mineral assemblage depend on the relative importances of the sinks of  $\text{SO}_2$ , as summarized in Fig. 3. Figure 3A shows the time evolution of the system with the photochemical sink removing 70% of all  $\text{SO}_2$  outgassed or produced by  $\text{H}_2\text{S}$  oxidation, whereas Fig. 3B is for 20% photochemical removal of  $\text{SO}_2$ . Atmospheric  $p\text{SO}_2$ , shown in the top graphs, is lower when the photochemical sink is important. This is due to the smaller overall size of the  $\text{S}^{4+}$  reservoir and despite water body acidification, which has the effect of increasing the vapor pressure of  $\text{SO}_2$  for a given reservoir size. Water body pH, shown in the middle graphs, is lower when photochemical production of  $\text{H}_2\text{SO}_4$  is sufficiently rapid, despite the decrease in  $p\text{SO}_2$ . Lastly, at higher relative photochemical destruction (sulfate production) rates, the mineral assemblage contains less siderite and a greater mole fraction of sulfate minerals, at the expense of sulfites, as shown in the bottom graphs. In all of our simulations,  $p\text{CO}_2$  rises because of the negligible precipitation of siderite. If precipitation of pyrite occurs, siderite may be altogether absent from the mineral assemblage (fig. S3). Sulfate minerals and  $\text{Mg}^{2+}$ -bearing minerals (whether sulfates or sulfites) are last to precipitate, leaving the aquatic reservoir relatively rich in  $\text{Mg}^{2+}$  and  $\text{SO}_4^{2-}$ . This has implications for the mineral assemblage that forms when such water bodies freeze or evaporate and is consistent with the observation that hydrated magnesium sulfate is an important phase on the surface of Mars (43). Our computations show that the pH and the concentrations of major rock-

forming cations in large water bodies can be controlled by equilibrium with  $\text{SO}_2$  and saturation of sulfite minerals, resulting in suppression of carbonate mineral precipitation.

Application of our hypothesis to martian history yields the following sequence of events: Volcanic outgassing of  $\text{CO}_2$ ,  $\text{SO}_2$ , and  $\text{H}_2\text{S}$  during the Noachian exhausted the oxidant supply, allowing  $\text{SO}_2$  to reach concentrations of a few ppm to several hundred ppm near the planet's surface. The partial pressure of  $\text{CO}_2$  increased gradually until it reached a critical level, perhaps during the period of most-rapid emplacement of Tharsis, when the combined radiative effect of  $\text{CO}_2$  and  $\text{SO}_2$  enabled the existence of liquid surface water. The  $\text{SO}_2$  climate feedback described above stabilized surface temperature, with precipitation of sulfite minerals from mildly acidic surface solutions preventing massive carbonate precipitation while allowing the formation of clays.

When volcanism subsided,  $\text{SO}_2$  was rapidly removed from the atmosphere by continued photolysis and by reaction with oxidants, now supplied at a faster rate than reduced gases. Without the radiative contribution of  $\text{SO}_2$ , the surface temperature dropped below the freezing point of water, surface water bodies froze, becoming more concentrated and precipitating the remaining ions in a progression of increasingly soluble salts. Water frozen at the surface was gradually redistributed by sublimation and refreezing because of seasonal cycling and changes in obliquity (44).

Under a now-oxidizing atmosphere, sulfite minerals at the surface would be episodically exposed to small amounts of surface or ground water and altered to sulfate, releasing acidity that would be stored in the soil. This oxidation of sulfites, in combination with oxidation of siderite and pyrite, is one possible way of creating the acidic environments proposed for later periods in martian history (45, 46) as well as the observed surface mineralogy. If the high volcanic flux persisted for  $10^8$  years accompanied by precipitation of sulfite minerals, elemental sulfur, and perhaps sulfides, then the supply of oxidants associated with hydrogen escape (16) would require about a billion years to transform all of the precipitates to sulfate. A shorter duration of clement conditions would imply a shorter oxidation time scale.

Despite subfreezing surface temperatures, the early geothermal gradient of Mars was high enough to maintain hydrothermal circulation in the crust (47). Subsurface silicate weathering coupled with carbonate mineral precipitation in crustal pores and fractures would have slowly removed the remaining atmospheric  $\text{CO}_2$ , consistent with the carbonate minerals found in veins in some martian meteorites (48). Estimates of martian crustal porosity (49) easily accommodate several bars of  $\text{CO}_2$ , sequestered in carbonate minerals. Three billion years of this process, in combination with atmospheric loss associated with large impacts and more efficient molecular escape after termination of the magnetic field of Mars, resulted in the present thin  $\text{CO}_2$  atmosphere.

Our hypothesis for a  $\text{SO}_2$  climate feedback successfully accounts for salient features observed on the surface of Mars and in the martian meteorites (13, 14, 41, 48, 50). Validation of our hypothesis would come from detection of sulfites on the martian surface, although the exclusion of sulfites from spectral libraries used for mineral detection on Mars, along with their tendency to oxidize, might make such detection difficult. Our hypothesis should apply to any planet with a reducing atmosphere and volcanically outgassed  $\text{SO}_2$  and may also explain the apparent scarcity of carbonate sediments in the Archean Earth (51).

## References and Notes

1. M. H. Carr, J. W. Head, *J. Geophys. Res.* **108**, 5042 (2003).
2. G. Neukum, B. A. Ivanov, W. K. Hartmann, *Space Sci. Rev.* **96**, 55 (2001).
3. D. L. Shuster, B. P. Weiss, *Science* **309**, 594 (2005).
4. J. B. Pollack, *Icarus* **91**, 173 (1991).
5. M. J. Newman, R. T. Rood, *Science* **198**, 1035 (1977).
6. R. J. Phillips *et al.*, *Science* **291**, 2587 (2001); published online 15 March 2001 (10.1126/science.1058701).
7. J. F. Kasting, *Icarus* **94**, 1 (1991).
8. F. Forget, R. T. Pierrehumbert, *Science* **278**, 1273 (1997).
9. Y. L. Yung, H. Nair, M. F. Gerstell, *Icarus* **130**, 222 (1997).
10. J. C. G. Walker, P. B. Hays, J. F. Kasting, *J. Geophys. Res.* **86**, 9776 (1981).
11. N. A. Morner, G. Etiopic, *Global Planet. Change* **33**, 185 (2002).
12. P. R. Christensen *et al.*, *J. Geophys. Res.* **106**, 23823 (2001).
13. B. C. Clark *et al.*, *Science* **194**, 1283 (1976).
14. A. S. Yen *et al.*, *Nature* **436**, 881 (2005).
15. E. V. Ballou, P. C. Wood, T. Wydeven, M. E. Lehwall, R. E. Mack, *Nature* **271**, 644 (1978).
16. H. Lammer *et al.*, *Icarus* **165**, 9 (2003).
17. J. Horita, M. E. Berndt, *Science* **285**, 1055 (1999).
18. J. C. Andrews-Hanna, R. J. Phillips, M. T. Zuber, *Nature* **446**, 163 (2007).
19. S. S. Johnson, M. T. Zuber, T. L. Grove, M. A. Mischna, in *Workshop on Martian Sulfates as Recorders of Atmospheric-Fluid-Rock Interactions*, Lunar and Planetary Institute, Houston, TX, 22 to 24 October 2006, abstr. no. 7038.
20. M. L. Coombs, T. W. Sisson, P. W. Lipman, *J. Volcanol. Geotherm. Res.* **151**, 19 (2006).
21. G. J. S. Bluth, C. C. Schnetzler, A. J. Krueger, L. S. Walter, *Nature* **366**, 327 (1993).
22. C. D. K. Herd, L. E. Borg, J. H. Jones, J. J. Papike, *Geochim. Cosmochim. Acta* **66**, 2025 (2002).
23. P. J. Wallace, I. S. E. Carmichael, *Am. Mineral.* **79**, 161 (1994).
24. F. P. Fanale, S. E. Postawko, *Lunar Planet. Sci. Conf.* **XXVI**, 391 (1995).
25. J. F. Kasting, K. J. Zahnle, J. P. Pinto, A. T. Young, *Origins Life Evol. Biosphere* **19**, 95 (1989).
26. L. V. Haff, in *Chemical Analysis*, J. H. Karchmer, Ed. (Wiley, New York, 1970), vol. 29, pp. 183–283.
27. A. F. Ryabinina, V. A. Oshman, *Tr. Ural. Lesotekh. Inst.* **28**, 182 (1972).
28. V. A. Krasnopolsky, *Icarus* **178**, 487 (2005).
29. K. Zahnle, R. M. Haberle, in *Workshop on Martian Sulfates as Recorders of Atmospheric-Fluid-Rock Interactions*, Lunar and Planetary Institute, Houston, TX, 22 to 24 October 2006, abstr. no. 7046.
30. K. J. Zahnle, J. C. G. Walker, *Rev. Geophys.* **20**, 280 (1982).
31. G. J. Molina-Cuberos, W. Stumptner, H. Lammer, N. I. Komle, *Icarus* **154**, 216 (2001).
32. A. S. Wong, S. K. Atreya, T. Encrenaz, *J. Geophys. Res.* **108**, 5026 (2003).
33. S. E. Postawko, W. R. Kuhn, *J. Geophys. Res.* **91**, D431 (1986).

34. The first and second acid dissociation constants of sulfuric acid are  $10^{-7.2}$  and  $10^{-1.85}$ , respectively, whereas those of carbonic acid are  $10^{-10.3}$  and  $10^{-6.3}$ .
35. Pre-industrial atmospheric  $p\text{SO}_2/p\text{CO}_2$  is  $\sim 3 \times 10^{-7}$ . However, sulfite minerals do not precipitate because Earth's ocean is not in equilibrium with these atmospheric concentrations. As soon as it dissolves, sulfite is either rapidly oxidized in the aqueous phase to sulfate or reduced by bacteria to sulfide.
36. R. G. Burns, *Geochim. Cosmochim. Acta* **57**, 4555 (1993).
37. A. Banin, F. X. Han, I. Kan, A. Cicelsky, *J. Geophys. Res.* **102**, 13341 (1997).
38. L. M. Mukhin, A. P. Koscheev, Y. P. Dikov, J. Huth, H. Wanke, *Nature* **379**, 141 (1996).
39. N. J. Tosca, S. M. McLennan, *Earth Planet. Sci. Lett.* **241**, 21 (2006).
40. A. G. Fairén, D. Fernandez-Remolar, J. M. Dohm, V. R. Baker, R. Amils, *Nature* **431**, 423 (2004).
41. F. Poulet *et al.*, *Nature* **438**, 623 (2005).
42. Surface reservoirs include the combined aquatic and atmospheric reservoirs.
43. A. Gendrin *et al.*, *Science* **307**, 1587 (2005); published online 17 February 2005 (10.1126/science.1109087).
44. B. M. Jakosky, R. M. Haberle, in *Mars*, H. H. Kieffer, Ed. (Univ. Arizona Press, Tucson, AZ, 1992), pp. 969–1016.
45. S. W. Squyres, A. H. Knoll, *Earth Planet. Sci. Lett.* **240**, 1 (2005).
46. A. H. Knoll *et al.*, *Earth Planet. Sci. Lett.* **240**, 179 (2005).
47. D. P. Schrag, M. T. Zuber, in *Sixth International Conference on Mars*, Pasadena, CA, 20 to 25 July 2003, abstr. no. 3113.
48. J. C. Bridges *et al.*, *Space Sci. Rev.* **96**, 365 (2001).
49. J. C. Hanna, R. J. Phillips, *J. Geophys. Res.* **110**, E01004 (2005).
50. J. P. Bibring *et al.*, *Science* **312**, 400 (2006).
51. A. B. Ronov, A. Yaroshev, *Geochem. Int.* **4**, 1041 (1967).
52. Discussions with J. Dufek, J. Dykema, W. Fischer, J. Higgins, P. Hoffman, M. Jellinek, S. Johnson, C. Langmuir, and S. Leroy contributed to this work. Support was provided by the NASA Planetary Geology and Geophysics Program and a Radcliffe Fellowship to M.T.Z., by the George Merck Fund of the New York Community Trust to D.P.S. and by a Harvard Origins of Life Initiative Graduate Fellowship to I.H.

26 June 2007; accepted 8 November 2007  
10.1126/science.1147039

## Coupled $^{142}\text{Nd}$ - $^{143}\text{Nd}$ Isotopic Evidence for Hadean Mantle Dynamics

Vickie C. Bennett,<sup>1,2\*</sup> Alan D. Brandon,<sup>3</sup> Allen P. Nutman<sup>4</sup>

The oldest rocks—3.85 billion years old—from southwest Greenland have coupled neodymium-142 excesses (from decay of now-extinct samarium-146; half-life, 103 million years) and neodymium-143 excesses (from decay of samarium-147; half-life, 106 billion years), relative to chondritic meteorites, that directly date the formation of chemically distinct silicate reservoirs in the first 30 million to 75 million years of Earth history. The differences in  $^{142}\text{Nd}$  signatures of coeval rocks from the two most extensive crustal relicts more than 3.6 billion years old, in Western Australia and southwest Greenland, reveal early-formed large-scale chemical heterogeneities in Earth's mantle that persisted for at least the first billion years of Earth history. Temporal variations in  $^{142}\text{Nd}$  signatures track the subsequent incomplete remixing of very-early-formed mantle chemical domains.

Isootope data for short-lived decay schemes such as the  $^{146}\text{Sm}$ - $^{142}\text{Nd}$  system [half-life ( $T_{1/2}$ ) 103 million years (My)] obtained from samples of the Moon, Mars, and meteorites are revealing the complexities of early planetary differentiation that occurred soon after accretion [e.g., (1–4)]. Attempts to demonstrate  $^{142}\text{Nd}$  variations in Earth were initiated in the 1990s (5), with recent measurements of some ancient rocks [dating from >3.6 billion years ago (Ga)] (6–10) now firmly establishing variable  $^{142}\text{Nd}/^{144}\text{Nd}$  ratios in Earth relative to modern terrestrial compositions. This is important because detectable  $^{142}\text{Nd}$  isotopic variations can only be generated from Sm/Nd fractionation during the largely unknown first ~300 My of Earth history, while  $^{146}\text{Sm}$  is still actively decaying. Previous studies focused largely on the ~3.7- to 3.8-billion-year (Gy)-old regions of the Isua supracrustal belt of West Greenland, representing largely one, albeit important, spatial and temporal point in Earth evolution. Interpreting the large range of reported  $^{142}\text{Nd}/^{144}\text{Nd}$  ratios [0 to +17 parts per million

(ppm) higher than modern terrestrial compositions] in terms of early planetary processes is complicated because many of the analyzed rocks were either metasedimentary mixtures of eroded terranes (7–9) or metabasalts (6, 9, 10) from areas that experienced widespread secondary chemical alteration [e.g., (11, 12)].

Tantalizing hints of Hadean Era (>4.0 Ga) Earth dynamics come from the recent recognition that all crust and upper mantle rocks today have a  $^{142}\text{Nd}/^{144}\text{Nd}$  excess of ~20 ppm compared with primitive chondritic meteorites (2, 13, 14), which were the building blocks of Earth. This requires not only that chemically distinct domains with high and low Sm/Nd, evolving to high and low  $^{142}\text{Nd}$ , respectively, formed during or soon after accretion but also that these domains must have persisted to the present in order to account for the continued isotopic offset between chondrites and modern terrestrial rocks. Additionally, the more extreme  $^{142}\text{Nd}$  excesses measured in some Archean rocks (6, 7, 9, 10) require the early existence of an older, or more severely depleted (higher Sm/Nd) mantle, whose extent and longevity is unknown. To track the origin, distribution, and interaction of these global chemical domains requires precise  $^{142}\text{Nd}$  data for ancient rocks with a range of ages and from a variety of localities.

Here, we present high-precision  $^{142}\text{Nd}$  data (Table 1) (15) combined with  $^{143}\text{Nd}$  data from samples of the two most aerially extensive >3.6-

Gy-old terranes: the 3000 km<sup>2</sup> Itsaq Complex (16) of southern West Greenland, of which the Isua supracrustal belt is one component, and the Narreyer Gneiss Complex of the Yilgarn craton, Western Australia. In contrast to previous studies, the emphasis is on analysis of the oldest tonalites, a juvenile granitic rock type typically representing the earliest formed continental crust in a region and from which direct age information in the form of U-Pb zircon ages can be obtained. Archean tonalites are melts of young oceanic crust [e.g., (17)], derived from the upper mantle. The intermediate basalt stage is likely short compared with the time scale of  $^{147}\text{Sm}$  decay and with Sm/Nd similar to that of the mantle source.

The Itsaq samples span a 210-My age range (3.64 to 3.85 Gy old) and include crystalline rocks from newly recognized localities of homogeneous 3.85-Gy-old tonalites (18) and >3.85-Gy-old mafic rocks (15). These samples are some of the oldest terrestrial rocks yet discovered. The two 3.73-Gy-old Narreyer Gneiss Complex tonalitic gneisses are the oldest rocks from the Australian continent (19). All rocks are from our field collections and represent the most geologically pristine materials, with well-defined crystallization ages having minimal secondary chemical alteration (table S1) (15).

Homogenized powdered samples weighing from 0.1 to 0.3 g were dissolved and processed to isolate >500 ng Nd. The  $^{142}\text{Nd}/^{144}\text{Nd}$  isotopic compositions were measured as Nd<sup>+</sup> on a Triton thermal ionization mass spectrometer using a multidynamic data collection scheme (9). Measurements of a standard Nd solution run interspersed with the samples yielded an external reproducibility (2 SD) of  $\pm 3.5$  ppm (fig. S1) (in-run precisions were from 1.0 to 2.5 ppm, 2 SE). Replicate analyses of 14 modern rocks yielded the same external precision as the standard data (fig. S2), which demonstrates the validity of this precision for chemically processed samples. The  $^{147}\text{Sm}-^{143}\text{Nd}$  data were obtained on separate powder samples using standard isotope-dilution methods (15).

Fifteen samples from the Itsaq Complex all have well-resolved  $^{142}\text{Nd}$  excesses of 9 to 20 ppm relative to the modern terrestrial reference composition (Table 1). The six basalts with ages

<sup>1</sup>Research School of Earth Sciences, The Australian National University, Canberra ACT, 0200 Australia. <sup>2</sup>Lunar and Planetary Institute, Houston, TX 77058, USA. <sup>3</sup>NASA Johnson Space Center, Mail Code KR, Houston, TX 77058, USA. <sup>4</sup>Institute of Geology, Chinese Academy of Geological Sciences, 26 Baiwanzhuang Road, Beijing, 100037, China.

\*To whom correspondence should be addressed. E-mail: vickie.bennett@anu.edu.au